University of Belgrade

Faculty of Physics

Ivanka Božović – Jelisavčić

Measurement of the semileptonic b branching fractions in the b reference frame with the DELPHI detector

– Ph.D. thesis summary –

VINCA Institute of Nuclear Sciences, Belgrade, Yugoslavia,

NCSR "Demokritos", Athens, Greece

Belgrade, July, 1999

The most of the research work presented in this thesis was done at the National Institute of Nuclear Physics in Padua (Istituto Nazionale di Fisica Nucleare/sezione di Padova), Italy, within the DELPHI group for inclusive lepton studies in b and c physics. Some of the results are completed in the Laboratory of physics, at the VINCA Institute of Nuclear Sciences in Belgrade.

1 Introduction

The presented analysis [15] is one of a few measurements of the semileptonic *b* branching fractions performed in the *b* reference frame. Making use of this particular approach, different from the other DELPHI analyses performed so far [1, 2], this analysis provides an interesting consistency cross check. It is worthy to note that there are no yet published results for the semileptonic branching fraction $BR(b \to \bar{c} \to l^-)$*.

A brief description of the DELPHI detector is given in section 2. The selection of the hadronic Z^0 decays along with a *b*-flavor tagging is described in section 3. The lepton selection and identification algorithms are discussed in section 4. Finally, the method of analysis and its results are presented in section 5.

2 The DELPHI detector

The DELPHI is a detector designed to provide high granularity over a 4π solid angle, and allowing powerful particle identification. The detector consists of a cylindrical section covering the barrel region of θ ($40^\circ < \theta < 140^\circ$) and two endcaps covering the forward regions. The superconducting solenoid provides uniform magnetic field of 1.23 T parallel to the z axis throughout the central tracking volume.

The time projection chamber (TPC) is the main tracking device. The TPC is a cylinder with a length of 3 m, an inner radius of 30 cm and an outer radius of 122 cm. Tracks are reconstructed using up to 16 space points in the region of polar angle: $39^\circ < \theta < 141^\circ$, and using at least 4 space points down to 21° and 159°.

The Outer and Inner detector in addition provide precise $R\Phi$ measurements in the plane perpendicular to the magnetic field. The Outer Detector (OD) consists of five layers of drift cells at radii between 198 cm and 206 cm covering the polar angle region from 42° to 138°. The Inner Detector (ID) is a cylindrical drift chamber with inner radius of 12 cm and outer radius of 28 cm. An average local track element precision is reaching a value of $\sigma(R\Phi) = 40\ \mu m$.

* The Review of Particle Physics for 1998 is not quoting a value of this branching fraction.

The micro-vertex detector (VD) consists of three concentric cylindrical layers of Si-strip detectors at radii of 6.3 cm, 9 cm and 11 cm from the interaction region, and they are called respectively: closer, inner and outer layer. It provides a precise reconstruction of the $R\Phi$ coordinates near the interaction region with an intrinsic resolution of $7.6\,\mu m$ for each layer. A single hit precision of the z coordinate depends on the polar angle, reaching a value of $9\,\mu m$ for the tracks perpendicular to the silicon modules. All three layers cover the polar angle region ($44^\circ < \theta < 136^\circ$), while the closer layer coverage goes down to 25°. The Micro-vertex detector, Inner Detector, Time Projection Chamber and Outer Detector are the most important elements of the tracking system of the DELPHI detector. In the forward region, the tracking is complemented by two sets of drift chambers (FCA and FCB) placed at distances of ± 165 cm and ± 275 cm from the interaction point.

The barrel electromagnetic calorimeter is the High Density Projection Chamber (HPC) which is a gas-sampling device that provides three-dimensional charge reconstruction. It covers the polar angles between 42° and 138°. In the forward region, electron and photon identification is provided by a led glass calorimeter (FEMC).

Muon identification is achieved by comparing the extrapolations of the reconstructed tracks with the hits in the Barrel (MUB) and Forward (MUF) muon drift chambers. They are covering polar angles between 53° and 127°, and between 11° and 45°, respectively. In the barrel region, a precision of the $R\Phi$ coordinate measurement is about 2 mm per each chamber, while a muon candidate track is reconstructed with the azimuthal angle precision of $\pm 1^\circ$. In the forward region, the tracks are reconstructed with the resolution in space coordinates of about 4 mm.

In this section, only detectors relevant for this analysis have been mentioned. A complete description of the DELPHI detector can be found in reference [3].

3 Event selection

Semileptonic b branching fractions are measured using the sample of 1236570 hadronic Z^0 decays in the 1994 data and 3069963 simulated events. The decays of Z^0 into hadrons were selected by requiring:

* a total energy of the charged particles larger than 15% of the center of mass energy;
* at least seven reconstructed charged particles.

Charged particles are accepted if: $|\cos(\theta_{track})| < 0.937$, their track length is larger than 30 cm, the momentum of a particle takes on value between 0.25 GeV/c and 45 GeV/c with a relative error less than 100%, the impact parameter of a charged particle relative to the interaction point is less than 5 cm in the plane perpendicular to the beam direction and less than 10 cm along the beam direction.

Showers detected in the FEMC, HPC and in the barrel hadronic calorimeter should have energy larger than 300 MeV, 500 MeV and 1000 MeV respectively, with relative errors less than 100%.

To assure a good b-tagging efficiency, the thrust axis of each event is restricted to the barrel region ($|\cos(\theta_{thrust})| < 0.80$) with a good vertex detector acceptance.

Simulated events are generated with the JETSET 7.4 event generator [4] and passed through the DELSIM program [5] that models the detector response. The simulated events are than processed through the same analysis chain as the real data. Jets were reconstructed using the JADE algorithm [6] with $Y_{cut}^{min} = 0.02$. The transverse momentum of the lepton was determined relative to the direction of the jet, with lepton excluded from a definition of the jet.

3.1 b-flavor tagging

To obtain a high purity *b* sample, the lifetime tagging [9] is applied. Events are divided into two hemispheres, with respect to the thrust axis, and the primary vertex is reconstructed in each hemisphere. The probability to originate from the primary vertex is calculated for each track by means of the impact parameter. Also, the probability $\mathrm{P_H}$ that hemisphere contains no secondary vertex is calculated. If the lepton is found in one hemisphere, the $\mathrm{P_H}$ of the opposite hemisphere is restricted to low values by criterion: $P_H < 0.001$.

For selecting different flavors, the following efficiencies are estimated from simulation: $\varepsilon_{ff}^{b} = 69.2\ \%$, $\varepsilon_{ff}^{c} = 12.9\ \%$ and $\varepsilon_{ff}^{u,d,s} = 1.1\ \%$, and the fraction of *b* events in the sample was found to be $P_b = 84.0\ \%$. The secondary vertex has been reconstructed on the basis of the inclusive charm reconstruction [10] using the lepton as a seed. It is found that the efficiency for reconstruction of the secondary vertex is 92.5% for the real data and 92.3% for the simulation. After the inclusive charm reconstruction, a *b* four-momentum is evaluated in the laboratory frame using the missing energy in the hemisphere and the reconstructed lepton four-momentum. The direction of the *b*-hadron is obtained by averaging the direction of the jet containing the lepton with the vector joining the primary to the secondary vertex. The resolution $\frac{\sigma(E_B)}{E_B} \approx 12\ \%$ is achieved.

4 The lepton sample

In this analysis, inclusive muons and electrons with momentum greater than 2 GeV/c are accepted. We selected tight muons [7] and electrons satisfying the *criterion 65* [8].

4.1 Muon identification

Muon identification is based on the quality of the extrapolation fit of a muon candidate track with respect to the hits in the muon chambers [7]. To exclude regions with poor geometrical acceptance, polar angle of a muon track was restricted to the intervals:

$$0.03 < \left|\cos\left(\theta_\mu\right)\right| < 0.62\,,$$

$$0.68 < \left|\cos\left(\theta_\mu\right)\right| < 0.95\,.$$

The muon efficiency was measured in $Z \to \mu^+\mu^-$ and $\tau \to \mu$ decays and in two-photon collisions $\gamma\gamma \to \mu^+\mu^-$. A mean efficiency of about 68% was found for tight muons in the barrel region [7]. Muon identification efficiency was used for data and Monte Carlo in the momentum dependent form [7].

An estimation of the misidentification probability was obtained by means of a lifetime-based anti *b*-tag, in order to select a background enriched sample. The hadron misidentification probability was found to be: (0.324 ± 0.023)%, (0.157 ± 0.003)$\%_{\mathrm{MC}}$ in the barrel, and (0.162 ± 0.041)%, (0.152 ± 0.004)$\%_{\mathrm{MC}}$ in the forward region [8]. The ratio of the hadron misidentification probability for the real and simulated events was found to be 2.19 ± 0.17 in the barrel, and 1.07 ± 0.28 in the forward region [8]. These ratios were used to reweight the simulated hadrons misidentified as muons.

4.2 Electron identification

Within the good acceptance region of the HPC ($|\cos(\theta_e)| < 0.72$), charged particle tracks are accepted as electron candidates on the basis of the information from the HPC, TPC and Ring Imaging CHerenkov detector that were used as a neural network [11] input. The network response was used to define a momentum dependent cut which would provide a constant 65% efficiency over the full momentum range (criterion 65) [8]. The efficiency of electron tagging was measured on a sample of Compton events and electrons produced from photon conversions. The ratio of the experimental efficiency to the simulated one is 0.93 ± 0.02 [8] and it was used for the proper reweighting of the simulated electrons.

The probability of tagging a hadron as an electron is measured in a background enriched sample by means of anti *b*-tagging. The hadron misidentification probability in data was found to be: (0.37 ± 0.03)%, and the ratio with the same quantity in simulated events is 0.74 ± 0.06 [8].

To reduce the contamination from electrons originating from photon conversions, electron tracks coming from the secondary vertex and carrying no transverse momentum to the direction from the primary to the secondary vertex were rejected.

4.3 Simulated lepton sample

In order to obtain the referent spectra from different sources of simulated leptons and to study the corresponding systematic effects, simulated leptons are classified with respect to their origin:

1. Direct *b* decays $(b \to l^-)$;
2. ″Wrong sign″ cascade *b* decays $(b \to c \to l^+)$;
3. ″Right sign″ cascade *b* decays $(b \to \bar{c} \to l^-)$;

4. Prompt leptons from J/ψ decays ($b \to J/\psi \to l^+ l^-$);
5. Leptons from $b \to \tau^- \to l^-$ decays;
6. Direct c decays $(c \to l^+)$;
7. Leptons from $c \to \tau^+ \to l^+$ decays;
8. Misidentified hadrons;
9. Leptons from light quark decays;
10. Leptons that do not originate from any of the sources mentioned above. This class of leptons is introduced for reason of completeness and is not statistically relevant.

The semileptonic *b* decays were simulated using the IGSW model [16].

3 Method of analysis and results

The semileptonic *b* branching fractions are measured by using lepton momentum spectra in the *b* reference frame. The resolution of the reconstructed lepton momentum was about 200 MeV/c. Lepton momentum spectra in the rest frame of the *b* quark are shown in Fig. 1.

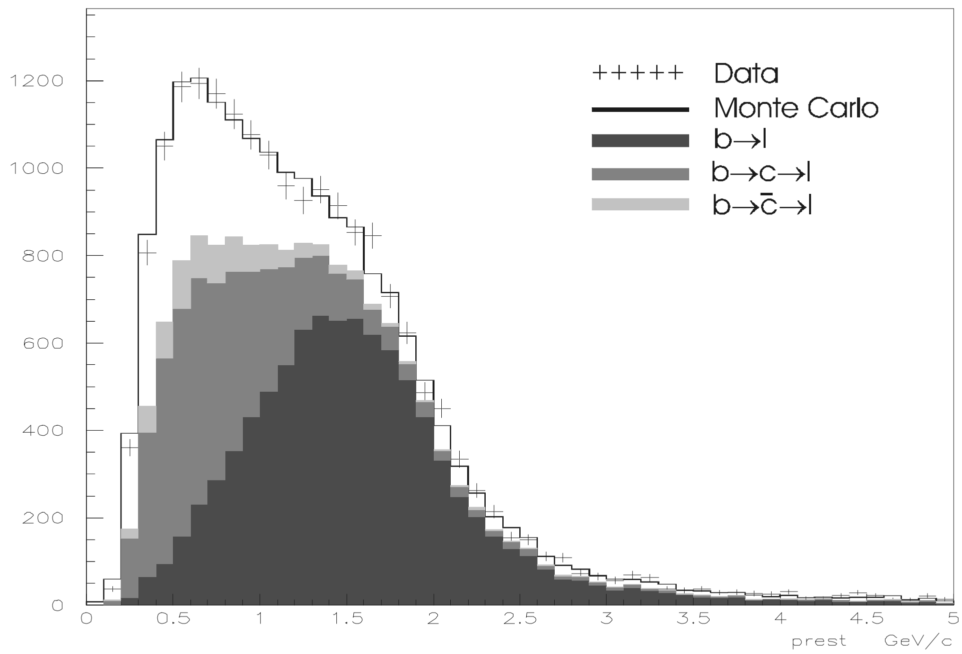

Figure 1. Lepton momentum distributions in the *b* quark reference frame.

Leptons from direct and cascade *b* decays are separated by means of the charge correlation that is defined as a product of lepton charge Q_L and the reconstructed jet charge of the opposite hemisphere Q_{OH} (see e.g.[12]):

$$\lambda = Q_L . Q_{OH} \tag{1}$$

The charge correlation indicates a correlation of lepton charge to the charge of the initial quark emitted in the opposite hemisphere. Thus the "right sign" leptons originating from $b \to l$ and $b \to \bar{c} \to l$ decays have the opposite correlation, while the "wrong sign" leptons from $b \to c \to l$ decays have the same correlation to the reconstructed jet charge of the opposite hemisphere. The charge correlation λ is used as a tagging variable in order to separate leptons of the right and wrong sign (Fig. 2). Discrimination power of this variable depends on several quantities related both to the *b* hadron production and decay mechanism and to the detector performance, which might be not well known.

In the two dimensional $\left(\lambda, p^l_{rest}\right)$ space the χ^2 is built and the lepton momentum distributions are fitted in order to measure the branching fractions $BR(b \to l)$, $BR(b \to c \to l)$ and $BR(b \to \bar{c} \to l)$. In each cell of the $\left(\lambda, p^l_{rest}\right)$ space the χ^2_{ij} is defined in the following way:

$$\chi^2_{ij} = \frac{(N^{Data}_{ij} - N^{MC}_{ij})^2}{\sigma^2_{ij}} \tag{2}$$

and the number of simulated leptons is corrected by introducing the fitting parameters *P* and δ :

$$N^{ij}_{MC} = (1+\delta_j) N^{ij}_{b\to l} \cdot P_{b\to l} + (1+\delta_{n_\lambda+1-j}) N^{ij}_{b\to c\to l} \cdot P_{b\to c\to l} + N^{ij}_{BCK} \tag{3}$$

$$N^{ij}_{MC} = (1+\delta_j) N^{ij}_{b\to l} \cdot P_{b\to l} + (1+\delta_{n_\lambda+1-j}) N^{ij}_{b\to c\to l} \cdot P_{b\to c\to l} + (1+\delta_j) N^{ij}_{b\to \bar{c}\to l} \cdot P_{b\to \bar{c}\to l} + N^{ij}_{BCK} \tag{4}$$

To conserve the number of leptons providing that they are only rearranged by invoking the delta parameters, the following condition is applied:

$$\sum_{j=1}^{n_\lambda} \delta_j \cdot \left(\sum_{i=1}^{n_{prest}} N^{ij}_{b\to l} \right) = 0 \tag{5}$$

The fits are performed using 4 λ and 25 p_{rest} cells. To minimize the overall χ^2, the MINUIT V94.1 program [13] was used.

In order to describe direct and cascade b decays and decays of the charmed hadrons, the Altarelli models [14] ACCMM and ALT2 have been used, respectively.

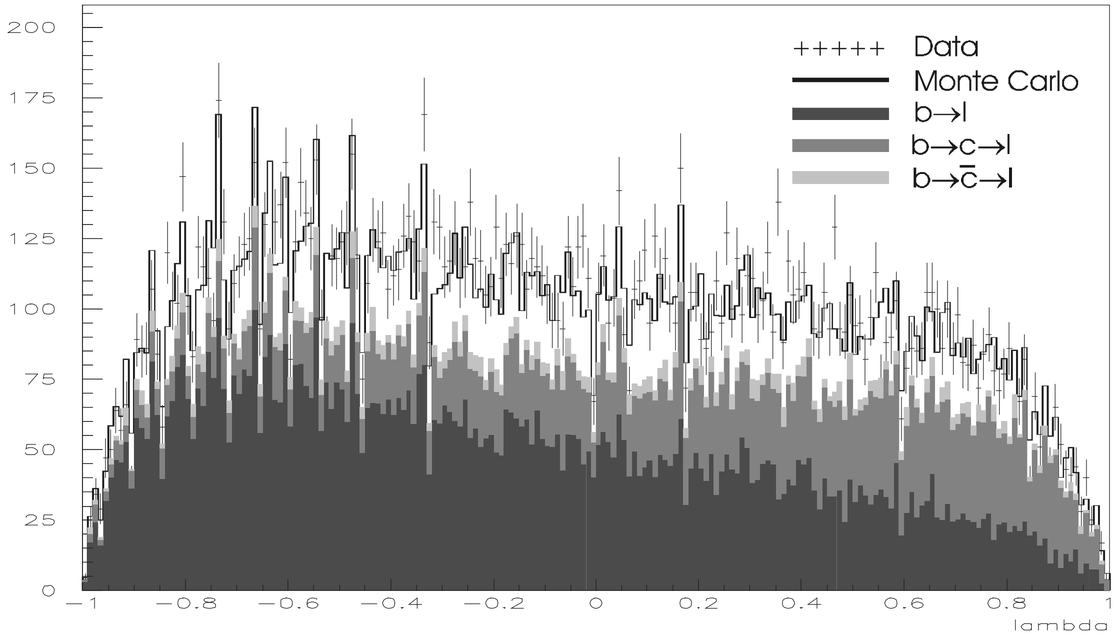

Figure 2. The charge correlation distributions for real data and the simulation.

5.1 Two-parameter fit

Performing a fit of the two branching fractions, the following results are obtained:

$BR(b \to l^-)$	$BR(b \to c \to l^+)$
$10.74 \pm 0.13(stat.)$	$8.43 \pm 0.22(stat.)$

Table 1. Results of the two-parameter fit to the 1994 lepton sample. The errors are statistical.

Considered sources of systematic uncertainty are given in table 2. The muon sample is given as an example.

Error source	**Variation**	$\Delta BR(b\to l^-)10^{-2}$	$\Delta BR(b\to c\to l^+)10^{-2}$
Identification efficiency	± 2 %	∓ 0.23	∓ 0.26
Misidentified leptons	± 10 %	∓ 0.02	∓ 0.24
Leptons from decays of the light quarks	± 10 %	< 0.01	∓ 0.16
Total uncorrelated error		**0.29**	**0.50**
leptons from $b\to\bar{c}\to l^-$	± 38.5 %	∓ 0.03	∓ 0.57
leptons from $b\to J/\psi\to l^+l^-$	± 28.5 %	∓ 0.04	< 0.01
leptons from $b\to\tau^-\to l^-$	± 16.4 %	∓ 0.02	∓ 0.07
leptons from $c\to l^+$	± 15 %	∓ 0.05	∓ 0.15
ε_{ff}^{c}	± 8 %	± 0.13	± 0.10
ε_{ff}^{uds}	± 20 %	± 0.03	± 0.02
Total correlated error		**0.15**	**0.60**
Total exp. systematic error		**0.28**	**0.71**
Decay model $b\to c\to l\quad(c\to l)$	$ALT1\ ^{+ALT2}_{-ALT3}$	- 0.10 + 0.08	- 0.05 < 0.01
Decay model $b\to l$	$ACCMM\ ^{+ISGW}_{-IG^{**}}$	- 0.28 + 0.44	+ 0.30 - 0.53
Total model error		**- 0.30** **+ 0.45**	**- 0.53** **+ 0.30**

Table 2. Summary of systematic uncertainties for the muon sample.

Lepton momentum distributions in the b reference frame after the fit was performed are shown in Fig 3. The corresponding values of the reduced χ^2 are 1.07 and 1.32, for the fit of muon and electron momentum distributions, respectively.

Performing the iterative procedure, the Peterson fragmentation parameter ε_b which best describes the data was determined. The iterative procedure was performed in the following way:

* the initial value of ε_b assumed to be the same as in the simulation ($\varepsilon_b=(0.2326\pm0.0010)\cdot10^{-2}$) was fixed and the branching fractions are fitted. Obtained results are shown in table 1.
* The branching ratios are fixed and the Peterson fragmentation parameter ε_b was fitted.

Convergence is reached after the first iteration and ε_b was found to be: $\varepsilon_b = (0.2441 \pm 0.0035) \cdot 10^{-2}$. The branching fraction results are not sensitive to 10% variation of the Peterson fragmentation parameter. Mean *b*-hadron energy $X_E = 0.7033 \pm 0.0004(stat.) \pm 0.004(sys.)$ corresponds to the fitted value of ε_b.

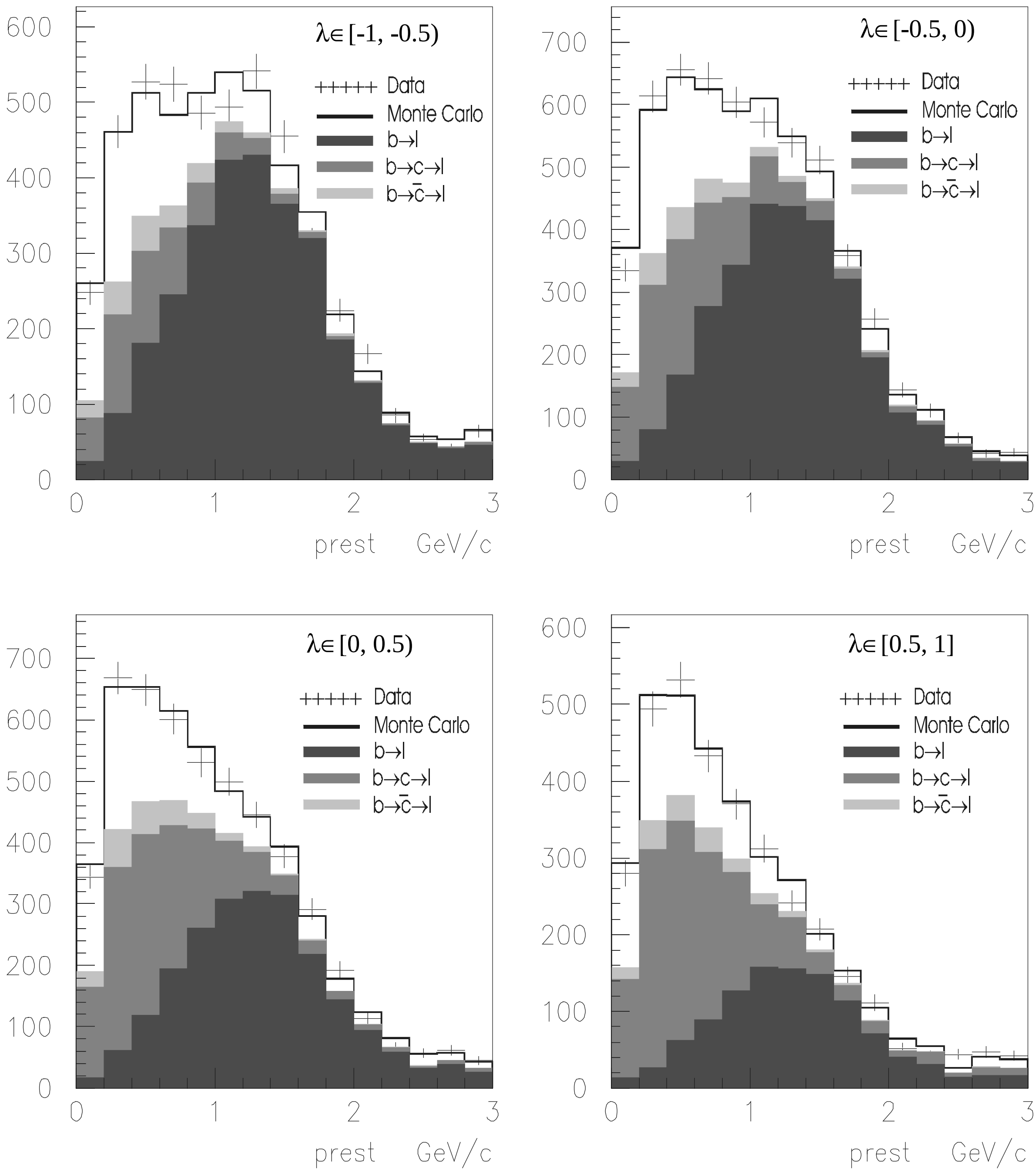

Figure 3. The muon momentum distributions in the *b* reference frame, after the fit was performed.

In conclusion, from a two-parameter fit of lepton momentum distributions in the *b* reference frame, the following results are obtained:

$$BR\left(b \to l^-\right) = (10.74 \pm 0.13(stat.) \pm 0.28(exp.sys.)\ {}^{+0.45}_{-0.30}(model))\%,$$

$$BR\left(b \to c \to l^+\right) = (8.43 \pm 0.22(stat.) \pm 0.84(exp.sys.)\ {}^{+0.32}_{-0.54}(model))\%.$$

5.2 Three-parameter fit

Performing a fit of the three semileptonic *b* branching fractions, the following results are obtained:

$BR(b \to l^-)$	$BR(b \to c \to l^+)$	$BR(b \to \bar{c} \to l^-)$
$10.68 \pm 0.14(stat.)$	$7.22 \pm 0.66(stat.)$	$2.00 \pm 0.45(stat.)$

Table 3. Results of the three-parameter fit to the 1994 lepton sample. The errors are statistical.

Corresponding values of the reduced χ^2 are 1.08 and 1.27, for the fit of muon and electron momentum distributions, respectively. The same sources of systematic error as in section 5.1 have been considered. The breakdown of the systematic errors is presented in table 4.

A three-parameter fit of lepton momentum distributions in the *b* reference frame, yields the following results:

$$BR\left(b \to l^-\right) = (10.68 \pm 0.14(stat.) \pm 0.27(exp.sys.)\ {}^{+0.50}_{-0.31}(model))\%,$$

$$BR\left(b \to c \to l^+\right) = (7.22 \pm 0.66(stat.) \pm 0.29(exp.sys.)\ {}^{+0.43}_{-0.25}(model))\%,$$

$$BR\left(b \to \bar{c} \to l^-\right) = (2.00 \pm 0.45(stat.) \pm 0.34(exp.sys.)\ {}^{+0.47}_{-0.73}(model))\%.$$

Error source	Variation	$\Delta BR\,(b \to l^-)$ 10^{-2}	$\Delta BR\,(b \to c \to l^+)$ 10^{-2}	$\Delta BR\,(b \to \bar{c} \to l^-)$ 10^{-2}
Identification efficiency	± 2 %	∓ 0.22	∓ 0.15	∓ 0.08
Misidentified leptons	± 10 %	< 0.01	∓ 0.05	∓ 0.15
Leptons from decays of the light quarks	± 10 %	< 0.01	< 0.01	∓ 0.13
Total uncorrelated error		**0.29**	**0.85**	**0.61**
leptons from $b \to J/\psi \to l^+ l^-$	± 28.5 %	∓ 0.08	< 0.01	∓ 0.22
leptons from $b \to \tau^- \to l^-$	± 16.4 %	∓ 0.01	± 0.05	∓ 0.09
leptons from $c \to l^+$	± 15 %	∓ 0.02	< 0.01	< 0.01
ε_{ff}^{c}	± 8 %	± 0.13	± 0.09	± 0.02
ε_{ff}^{uds}	± 20 %	± 0.03	± 0.02	< 0.01
Total correlated error		**0.16**	**0.10**	**0.24**
Total exp. systematic error		**0.27**	**0.19**	**0.32**
Decay model $b \to c \to l \quad (c \to l)$	$ALT1\ {}^{+ALT2}_{+ALT3}$	- 0.10 + 0.07	< 0.01 + 0.07	- 0.02 + 0.02
Decay model $b \to l$	$ACCMM\ {}^{+ISGW}_{-IG^{**}}$	- 0.31 + 0.50	- 0.23 + 0.41	+ 0.44 - 0.73
Total model error		**- 0.33** **+ 0.50**	**- 0.23** **+ 0.42**	**- 0.73** **+ 0.44**

Table 4. Summary of systematic uncertainties for the muon sample.

6 Conclusion

From a fit of lepton momentum distributions in the b reference frame, using the data collected with the DELPHI detector during 1994, the semileptonic b branching ratios $BR(b \to l^-)$, $BR(b \to c \to l^+)$ and $BR(b \to \bar{c} \to l^-)$ have been measured. A fit of the two and three branching fractions is performed and the following results are obtained:

$$BR\left(b \to l^-\right) = (10.74 \pm 0.13(stat.) \pm 0.28(exp.sys.)\ {}^{+0.45}_{-0.30}(model))\%,$$

$$BR\left(b \to c \to l^+\right) = (8.43 \pm 0.22(stat.) \pm 0.84(exp.sys.)\ {}^{+0.32}_{-0.54}(model))\% \text{ and}$$

$$BR\left(b \to l^-\right) = (10.68 \pm 0.14(stat.) \pm 0.27(exp.sys.)\ {}^{+0.50}_{-0.31}(model))\%,$$

$$BR\left(b \to c \to l^+\right) = (7.22 \pm 0.66(stat.) \pm 0.29(exp.sys.)\ {}^{+0.43}_{-0.25}(model))\%,$$

$$BR\left(b \to \bar{c} \to l^-\right) = (2.00 \pm 0.45(stat.) \pm 0.34(exp.sys.)\ ^{+0.47}_{-0.73}(model))\%.$$

With respect to the uncorrelated errors, the results for the $BR(b \to l^-)$ and $BR(b \to c \to l^+)$, are in agreement better than 1.5 standard deviations and they are consistent with results of the previous DELPHI analyses performed in the laboratory frame [1,2]. Because of its specific approach, this analysis is providing an important consistency cross check. As can be seen, uncertainties that are related to the applied heavy quark decay models are still significant. It was not possible to distinguish between different decay models on the basis of the reduced χ^2 values.

Acknowledgements

I would like to thank Dr. Franco Simonetto from the National Institute of Nuclear Physics, from Padua, Italy (*Istituto Nazionale di Fisica Nucleare/sezione di Padova*), where the most of this research was done. Also, I would like to thank all the colleagues from the DELPHI group for lepton studies in *b* and *c* physics, in particular, Dr. Martino Margoni who contributed to this analysis, not only through his work on tuning of lepton identification, but with many useful comments and observations, as well. I am also indebted to Dr. Petar Adzic from the VINCA Institute of Nuclear Sciences from Belgrade, who supervised my work on this thesis. Finally, this research would not be possible without support of DELPHI group from the NSCR "Demokritos".

References

1. *M. Calvi, P. Ronchese,* DELPHI Collaboration, DELPHI 97-118 CONF 100, 1997.
2. *M. Calvi, E. Cortina, V. Lara, F. Martinez-Vidal, J. Salt, Ch. de la Vaissière, I. Bozovic*, DELPHI 98-122 CONF 183, presented at the International Conference on High Energy Physics (ICHEP ′98), Vancouver, Canada, 1998.
3. *P. Abreu et al*., DELPHI Collaboration, Nucl. Inst. Meth. **A378** (1996) 57.
4. *T. Sjöstrand et al*., Z physics at LEP 1, CERN89-08, 1989.

5. DELSIM Reference manual, DELPHI 87-98/PROG 100, 1989.
6. *W. Bartel et al.*, JADE Collaboration, Z. Phys. **C33** (1983) 23;
S. *Bethke et al.*, Phys. Lett. **B213** (1988) 235.
7. *F. Stichelbaut, G. Wilkinson*, Performance of Muon Identification in DELPHI for 93 and 94 Data, DELPHI 95-140 PHYS 565, 1995.
8. *M. Margoni* (DELPHI/INFN Padova), private communication.
9. *G.V. Borisov*, DELPHI Collaboration, Lifetime Tag of events $Z^0 \to b\bar{b}$ with the DELPHI detector, DELPHI Note, 11. August, 1994.
10. *P. Abreu et al.*, DELPHI Collaboration, A precise measurement of the B_d^0 meson lifetime using a new technique, CERN-PPE/96-139, 1996.
11. *C. Kreuter*, Electron Identification using a Neural Network, DELPHI 96-169 PHYS 658, 1996.
12. *P. Antilogus et al.*, DELPHI Collaboration, Measurement of the Forward-Backward Asymmetries of $e^+e^- \to Z \to b\bar{b}$ and $e^+e^- \to Z \to c\bar{c}$, DELPHI 95-87 PHYS 522, 1995.
13. *F. James*, MINUIT V94.1, CERN Program Library Long Writeup **D506**, 1994.
14. *G. Altarelli, S.Petrarca*, Phys. Lett. **B21** (1991) 303.
15. *P. Antilogus, I. Bozovic, M. Calvi, E. Cortina, Ch. de la Vaissière, M. Feindt, V. Lara, F. Martinez-Vidal, M. Margoni, J. Salt, F. Simonetto, P. Ronchese, J. Yi,* Measurement of the semileptonic *b* branching ratios in *Z* decays, Paper (DELPHI 99-111 CONF 298) submitted to the HEP'99 Conference, Tampere, Finland, 1999.
16. *N. Isgur, M. Wise*, Phys. Lett. **B232** (1989) 113; **B237** (1990) 527.